HOKKAIDO UNIVERSITY

Title	Nb-Gateway for Hydrogen Desorption in Nb2O5 Catalyzed MgH2 Nanocomposite
Author(s)	Ma, Tao; Isobe, Shigehito; Wang, Yongming et al.
Citation	Journal of Physical Chemistry C, 117(20), 10302-10307 https://doi.org/10.1021/jp4021883
Issue Date	2013-05-23
Doc URL	https://hdl.handle.net/2115/53026
Type	journal article
File Information	jp4021883.pdf



Hokkaido University Collection of Scholarly and Academic Papers : HUSCAP

THE JOURNAL OF PHYSICAL CHEMISTRY C

Article

pubs.acs.org/JPCC

Nb-Gateway for Hydrogen Desorption in Nb_2O_5 Catalyzed MgH_2 Nanocomposite

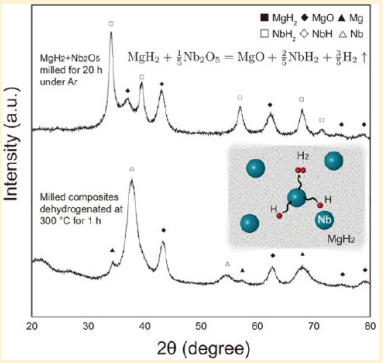
Tao Ma,*[,†] Shigehito Isobe,*[,†,‡] Yongming Wang,[†] Naoyuki Hashimoto,[†] and Somei Ohnuki[†]

[†]Graduate School of Engineering, Hokkaido University, N-13, W-8, Sapporo 060-8628, Japan

[‡]Creative Research Institution, Hokkaido University, N-21, W-10, Sapporo, 001-0021, Japan

Supporting Information

ABSTRACT: The state of Nb-contained catalysts in MgH_2 nanocomposites was investigated during the full cycle. X-ray diffraction (XRD) results showed that Nb_2O_5 and Nb reacted with MgH_2 during ball-milling, forming NbH_2 and NbH, respectively. In the following dehydrogenation, the (di)hydride decomposed, and Nb was produced. Then NbH was generated in both samples after rehydrogenation. Similar composition in both samples suggests that the catalytic effect follows the same mechanism, the Nb-gateway model, in which Nb facilitates the hydrogen transportation from MgH_2 to the outside. By contrast, NbO remained during the full cycle. Scanning and transmission electron microscopy (SEM and TEM) observations revealed that the Nb_2O_5-doped sample tended to be refined in size, compared to the Nb-doped and NbO-doped ones. Nb crystals in the Nb_2O_5-doped sample were observed to be highly dispersed in the sample, with 10−20 nm in size. Given all that, tiny Nb crystals distributed in the composites worked as the gateway facilitating hydrogen transportation and improving dehydrogenation properties.



INTRODUCTION

Hydrogen is a promising alternative energy carrier because of its prominent advantages such as high energy density, great variety of potential sources, light weight, and environmental friendliness; thus it has been highly regarded. As a medium for hydrogen storage, magnesium hydride has been well studied in the past decades. Having notable advantages such as high capacity (7.6 mass %), light weight, and low cost, it is considered as a promising candidate for hydrogen storage materials.[1] However, the absorption and desorption processes require high temperatures of 300−400 °C, and the reactions are slow. By ball-milling with some transition metals, the kinetics of the reactions can be improved.[2−4] Huot et al. showed the result that MgH_2 nanoparticles catalyzed by 5 mol % Nb completed full desorption within 300 s at 300 °C.[4] They confirmed the formation of a short-lived metastable NbH_x ($x \approx 0.6$) phase during dehydrogenation, thus concluded that it acted as a gateway through which hydrogen from MgH_2 released.[5] A similar mechanism was claimed later by Li et al. in a density functional theory calculation, in which the substitution of Nb at the Mg site followed by the clustering of H around Nb was a likely pathway for hydrogen desorption.[6] On the other hand, Mg−Nb−O perovskite phase was also found in the dehydrogenated composite and believed to help with hydrogen transportation.[7]

Transition-metal oxides also show the catalytic effect on facilitating hydrogen absorption and desorption in nanostructured MgH_2.[8−13] Among those catalysts studied so far, Nb_2O_5 showed a superior catalytic effect. Barkhordarian et al. reported that MgH_2 catalyzed by 0.5 mol % Nb_2O_5 and ball-milled for 100 h finished desorption within 90 s at 300 °C.[10] Hanada et al. reported that the composite, MgH_2 and 1 mol % Nb_2O_5 milled for 20 h, was able to absorb ∼4.5 wt % of hydrogen after full desorption, under a pressure of 1.0 MPa within 15 s at room temperature.[13] However, the exact mechanism leading to this remarkable catalytic effect is still unclear. In the recent transmission electron microscopy (TEM) observations, the size of both MgH_2 and Nb_2O_5 was found to be within nanoscale. Thus the refinement of size and the consequently homogeneous distribution of the additives may be responsible for the fast kinetics.[14,15] It was also confirmed that in the cycled composites, Mg−Nb−O phases formed, which accelerated hydrogen desorption by providing special diffusion pathways.[16,17]

In our previous investigation on the chemical bonding state of Nb in Nb_2O_5 catalyzed MgH_2 nanocomposites, it was found that Nb_2O_5 was gradually reduced as the ball-milling time increased. The reduced Nb compounds were considered as the essential catalysts improving the desorption kinetics.[18] In the present paper, we aimed at clarifying the exact state of the catalyst during a full cycle. The reactions between MgH_2 and three kinds of Nb-contained catalysts, Nb, NbO, and Nb_2O_5, were investigated and compared, in order to figure out the mechanism of the catalytic effect. We increased the amount of the additives to 50 wt % so that we were able to identify the state of the additives exactly at each stage. The morphology and

Received: March 4, 2013
Revised: April 29, 2013
Published: May 1, 2013

 © 2013 American Chemical Society dx.doi.org/10.1021/jp4021883 | J. Phys. Chem. C 2013, 117, 10302−10307

the microstructure of the samples were also compared to draw the conclusion.

EXPERIMENTAL SECTION

MgH_2 powder was purchased from Alfa Aesar with a purity of 98%. Powder of Nb_2O_5 (99.99%), NbO (99.9%), and Nb (99.9%) was purchased from the Kojundo Chemical Laboratory. All materials were used as received. For sample preparation, 150 mg MgH_2 and 150 mg additives (Nb_2O_5, NbO or Nb) were sealed into a steel vessel (30 cm^3 inner volume) together with 20 steel balls (7 mm in diameter). After evacuating the vessel, 1 MPa Ar was introduced into it. The mixture was mechanically milled at 400 rpm for 20 h using a planetary ball-milling apparatus (Fritsch P7). Dehydrogenation was performed by annealing the milled composites for 1 h at 300 °C under vacuum. Rehydrogenation was carried out at 200 °C for 2 h, under a 1 MPa H_2 atmosphere. X-ray diffraction (XRD) was performed at each stage, using a Philips X'Pert Pro powder diffractometer with Cu K_α radiation. The morphology of the samples was observed via a field emission scanning electron microscope (FE-SEM, JEOL JSM-6500F). TEM observations were carried out using a 200 kV TEM (JEOL JEM-2010) and a 1250 kV high-voltage electron microscope (HVEM, JEM-ARM1300). The plastic bag method[19] was used to prevent oxidation of the samples during transport into TEM instruments.

RESULTS AND DISCUSSION

State of the Additives during the Full Cycle. Figure 1 shows the XRD profiles of MgH_2–Nb_2O_5 nanocomposite

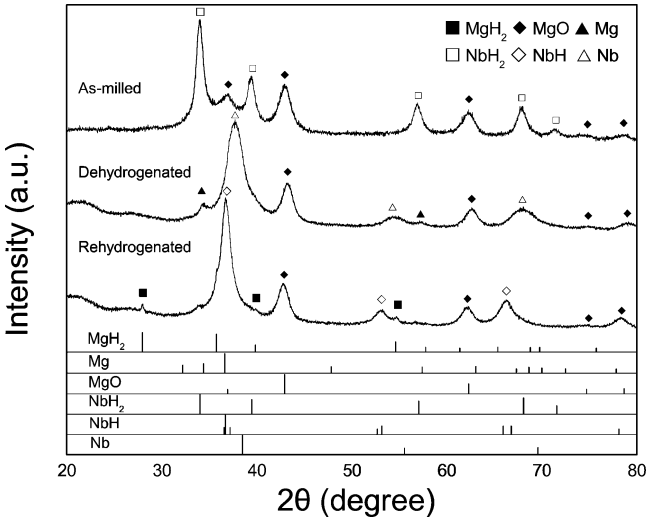


Figure 1. XRD profiles of MgH_2–Nb_2O_5 nanocomposites.

during the full cycle. In the as-milled sample, Nb_2O_5 was not detected. Instead, the peaks from NbH_2 and MgO can be seen, indicating that Nb_2O_5 reacted with MgH_2 during the ball-milling process. Nb (II) hydride and MgO as the products of the reaction were generated then. The reaction equation can be written as follows:

$$MgH_2 + \frac{1}{5}Nb_2O_5 = MgO + \frac{2}{5}NbH_2 + \frac{3}{5}H_2\uparrow \quad (1)$$

Equation 1 explains the common phenomenon that MgO is always found in the milled MgH_2–Nb_2O_5 composite. Additionally, the reduction of Nb_2O_5 agrees with our previous work,[18] implying that the reduction product, NbH_2, may be the essential catalyst that improves the desorption kinetics. According to the mole ratio of the reactants, a small amount of MgH_2 should remain after ball-milling. The absence of the peaks of MgH_2 suggests that the residual MgH_2 is microcrystalline. In the dehydrogenated sample, since both MgH_2 and NbH_2 have decomposed, the XRD profile shows the coexistence of Mg, Nb, and MgO. After rehydrogenation, the peaks of MgH_2 and NbH were confirmed in the XRD profile. It indicates that, after one cycle, the initial additive, Nb_2O_5, was converted into the niobium(I) hydride state.

Similar reactions were found in the MgH_2–Nb nanocomposite, except that NbH rather than NbH_2 appeared after ball-milling, as shown in the XRD profiles in Figure 2. The

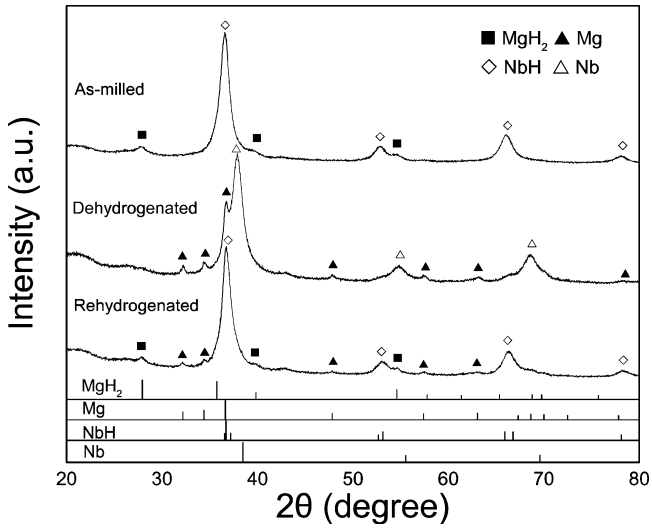


Figure 2. XRD profiles of MgH_2–Nb nanocomposite.

initial additive was changed into NbH following the equation below:

$$MgH_2 + Nb = 2NbH + Mg \quad (2)$$

This result is consistent with the work of Huot et al., in which NbH was also found in the 5 mol % Nb catalyzed MgH_2 nanocomposite.[4] The dehydrogenation resulted in the formation of Mg and Nb. Finally, the metals returned to MgH_2 and NbH state after rehydrogenation.

Figure 3 shows the XRD profiles of the NbO-doped sample during the full cycle. Unlike the obvious interactions between MgH_2 and the additives in the previous ones, MgH_2 and NbO still remained after ball-milling. After dehydrogenation, the peaks of Mg were seen, due to the decomposition of MgH_2. The latter reappeared after rehydrogenation. Comparing the XRD profiles during the whole cycle, the peaks from NbO did not change at all. As an aside, an unknown peak at $2\theta = 44°$, which is close to β-MgO (400), appeared during the full cycle. We have not found any description about the metastable β-MgO in the literature. Whether it helps the dehydrogenation or not is unclear.

Mechanism of the Catalytic Effect in MgH_2–Nb_2O_5 Nanocomposite. It must be pointed out that in both Nb_2O_5-doped and Nb-doped samples, the peaks of Nb in the XRD spectra of the dehydrogenated samples were a little shifted toward the lower angle. The positions, however, quite match

dx.doi.org/10.1021/jp4021883 | J. Phys. Chem. C 2013, 117, 10302–10307

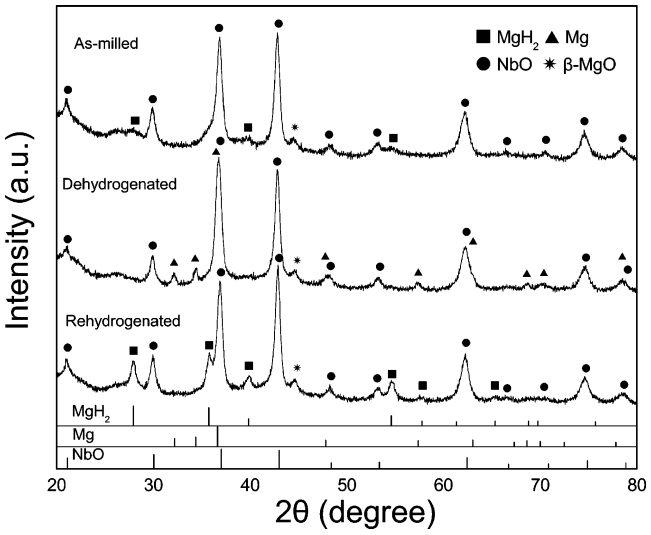


Figure 3. XRD profiles of MgH_2−NbO nanocomposite.

the metastable NbH_x phase, which is a solid solution described in the references.[5,20] For one thing, it reaffirms the gateway model that NbH_x facilitates the hydrogen transportation in MgH_2−Nb composites, described elsewhere.[4,5] For another, it suggests the possibility that the Nb_2O_5-doped sample may also undergo a dehydrogenation process following the Nb-gateway model, resulting in the formation of NbH_x solid solution as it does in the Nb-doped sample.

Comparing the XRD results of Nb_2O_5-doped and Nb-doped samples, it can be noticed that the composition was the same after one cycle, except that MgO as the byproduct of the reaction existed in the former. The role of MgO was investigated additionally. (Details can be found in the Supporting Information.) The dehydrogenation peak-temperatures in Nb-doped and Nb-MgO-doped samples are almost the same (254 and 257 °C, respectively, shown in Figure S1), revealing that the addition of MgO, though it makes the same composition as in the Nb_2O_5-doped sample, provided no contribution to the desorption property. Furthermore, SEM observations shown in Figure S2 present few changes in the morphology brought by the addition of MgO, compared to the Nb-doped sample. Both the results indicate that the existence of MgO is meaningless for the desorption properties. Therefore, we can safely conclude that the catalytic effect in MgH_2−Nb_2O_5 nanocomposites is attributed to the existence of Nb, as it does in the Nb-doped composite. In both samples, the catalytic effect follows the same mechanism during dehydrogenation, which is based on a Nb−gateway model for hydrogen release. First, niobium (di)hydride decomposes rapidly (because niobium hydride is thermodynamically unstable) and Nb forms. Then, hydrogen diffuses from MgH_2 to Nb, forming the NbH_x solid solution. This metastable phase is stabilized by the hydrogen flow from MgH_2 to the outside, until MgH_2 exhausts finally. In both samples, Nb plays an important role in hydrogen transportation and acts as an essential catalyst improving the kinetics during dehydrogenation.

The Size Effect in the Desorption. As we stated that the catalytic effect of Nb_2O_5 and Nb follows the same mechanism, the Nb-gateway model, one would doubt why Nb_2O_5-doped and Nb-doped samples exhibited different desorption properties (see Figure S1). In order to figure out the differences between them, we estimated the crystallite size of MgH_2 in the as-milled samples, as well as that of Mg and Nb after dehydrogenation, using the Scherrer equation:

$$\tau = \frac{K\lambda}{\beta \cos\theta} \tag{3}$$

where K is the shape factor, typically 0.89, λ is the X-ray wavelength, 1.54 Å for Cu radiation, β is the full width at half-maximun (fwhm), θ is the Bragg angle, and τ is the mean size of the crystallites.[21] For the estimation of MgH_2, we selected the strongest peak, MgH_2 (110), to apply eq 3. In the case of Mg and Nb, (110) and (200), respectively, rather than the strongest peaks were chosen, in order to avoid the peak overlapping. The measured fwhm and corresponding crystallite size are listed in Table 1. The size of MgH_2 in the Nb-doped and NbO-doped samples after ball-milling was around 70 Å, while that in the Nb_2O_5-doped sample was microcrystalline, since the peak was not detected in the XRD spectrum. Therefore, the size of MgH_2 in the Nb_2O_5-doped sample is extremely smaller than those in the others. The size of Nb and Mg in the Nb_2O_5-doped sample after dehydrogenation was evaluated as 38 Å and 88 Å respectively, roughly half those in the Nb-doped sample (68 Å and 190 Å, respectively). It was suggested that when MgH_2 is milled with Nb_2O_5, the crystallites tend to be refined. The decrease in size can lead to a fast decomposition, thus partially explaining the better desorption property of the Nb_2O_5-doped sample, compared to the others. On the other hand, being comparable in size compared to the Nb-doped sample, the NbO-doped sample showed better desorption property. It implies that there are other factors determining the desorption kinetics in the NbO-doped sample.

In order to compare the morphology of the composites, we observed the as-milled and hydrogenated samples by SEM. The typical images are shown in Figure 4. It can be seen that for all the composites, the morphology hardly changed after dehydrogenation. On the other hand, the difference in size can be seen obviously. The Nb_2O_5-doped sample shown in Figure 4a,d is distinctly small in size, while the particle size in the other two is much bigger than the former. It indicates that both MgH_2 and the additive could be pulverized more easily in the Nb_2O_5-doped composite. The same tendency was also observed in 1 mol % Nb_2O_5-doped and 2 mol % Nb-doped, as well as 2 mol % NbO-doped samples, as shown in Figure S2. This could be explained by the physical properties of the additives. As a ceramic, Nb_2O_5 exhibits hard and brittle

Table 1. Crystalline Size (τ; in Å) of MgH_2, Mg, and Nb in Each Sample

	Nb_2O_5-doped		Nb-doped		NbO-doped	
peak	fwhm (°)	τ (Å)	fwhm (°)	τ (Å)	fwhm (°)	τ (Å)
MgH_2 (110) as-milled	undetectable	microcrystalline	1.086	76	1.121	73
Nb (200)	2.367	38	1.232	68		
Mg (110)	1.029	88	0.487	190	0.639	143

dx.doi.org/10.1021/jp4021883 | J. Phys. Chem. C 2013, 117, 10302−10307

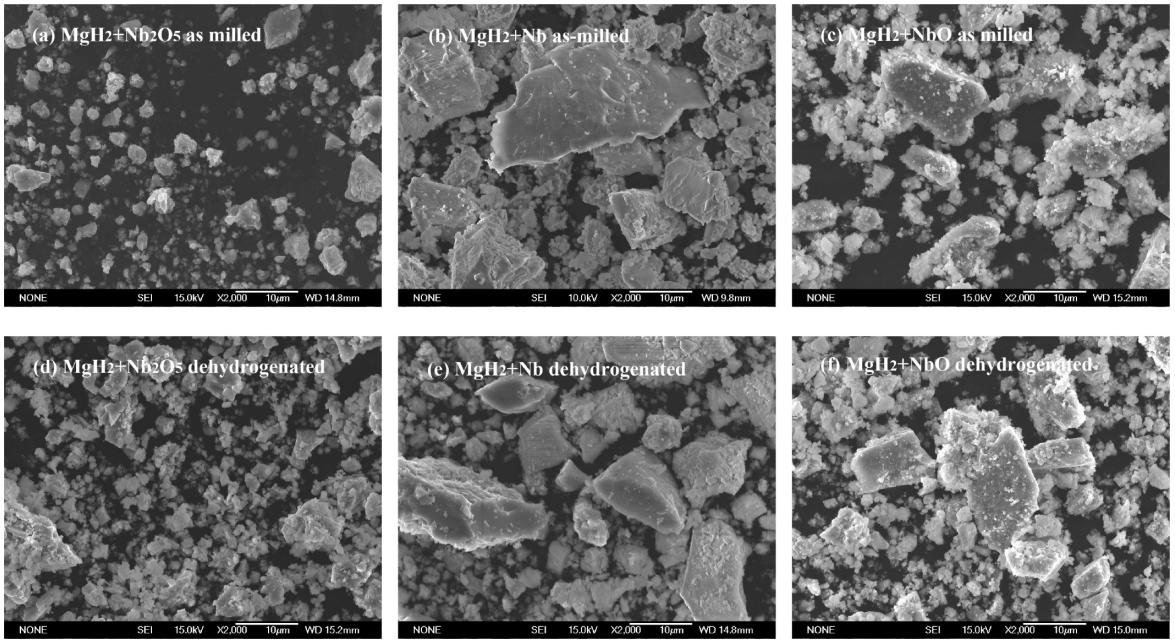


Figure 4. SEM images showing the morphology of the as-milled and dehydrogenated composites.

character, while Nb metal and NbO, which show metallic properties, are ductile and not easy to be pulverized. Thus even though following the same mechanism during dehydrogenation as Nb_2O_5-doped and Nb-doped composites are, the smaller size leads to a faster reaction rate. In other words, the size effect is considered to play an important role during the catalyst-promoted dehydrogenation.

Figures 5 and 6 show the typical TEM images of the Nb_2O_5-doped and Nb-doped composites after dehydrogenation. The

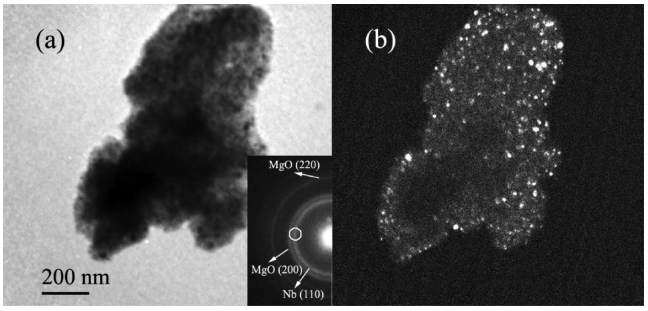


Figure 5. Typical TEM micrograph of the Nb_2O_5-doped composite after dehydrogenation. (a) Bright field image. (b) Corresponding dark field image taken from the circled area.

insets in both figures show the Debye rings of Nb, meaning that Nb is polycrystalline. Nb crystals can be seen in the dark field images taken by selecting parts of Nb (110) rings marked by the white circles in the diffraction pattern. For the Nb_2O_5-doped sample as shown in Figure 5b, it can be seen that Nb crystals, with a size around 10−20 nm, dispersed homogeneously in the Mg matrix. However, in the case of the Nb-doped sample, Nb crystals with a size of ∼100 nm can be observed, as shown in Figure 6b. We also found Nb single-crystals with a size around 200 nm, shown in Figure 7. The inhomogeneity in the size of the Nb catalyst could hinder the catalytic effect and deteriorate the desorption properties.

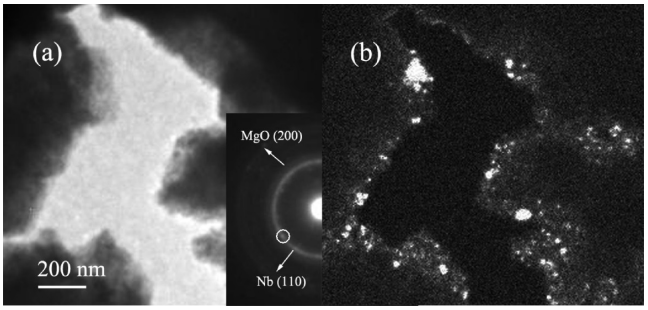


Figure 6. Typical TEM micrograph of the Nb-doped composite after dehydrogenation. (a) Bright field image. (b) Corresponding dark field image taken from the circled area.

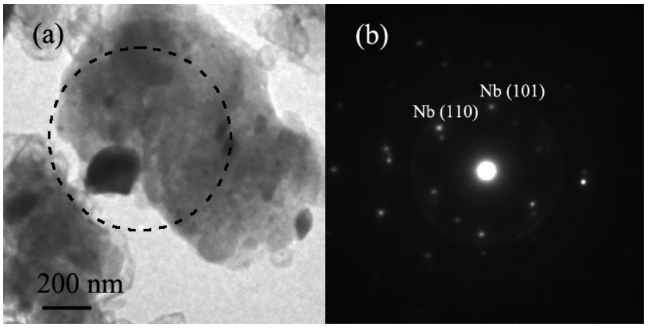


Figure 7. TEM images showing Nb particles in the Nb-doped composite after dehydrogenation. (a) Bright field image. (b) Diffraction pattern from the circled area.

Taking advantage of high-resolution electron microscopy, we were able to confirm the existence and the size of NbH_2 and Nb in the 1 mol % Nb_2O_5-doped composite. Figure 8a shows the high resolution image of the 1 mol % Nb_2O_5-doped composite before dehydrogenation. In the fast Fourier-transformation (FFT) image (Figure 8b) taken from the selected area, a pair of spots corresponding to NbH_2 (111) was identified. The size of NbH_2 was around 20 nm, as can be seen in the inverse fast

dx.doi.org/10.1021/jp4021883 | J. Phys. Chem. C 2013, 117, 10302−10307

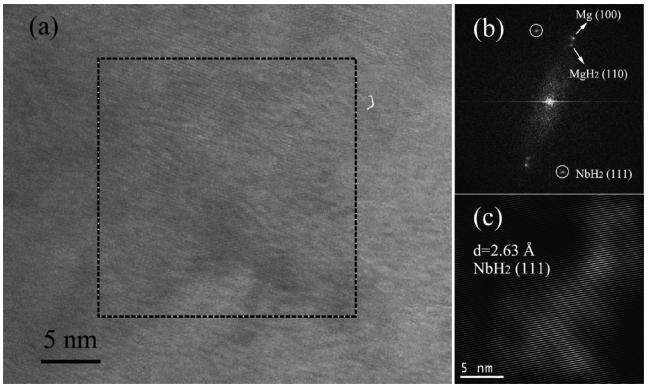


Figure 8. (a) High-resolution image, (b) FFT, and (c) IFFT images of the MgH_2 and 1 mol % Nb_2O_5 composite after ball-milling. The FFT area is marked by the square in panel a.

Fourier-transformation (IFFT) image shown in Figure 8c. The high-resolution image of the dehydrogenated sample is presented in Figure 9a. Similarly, the spots of Nb (110) were

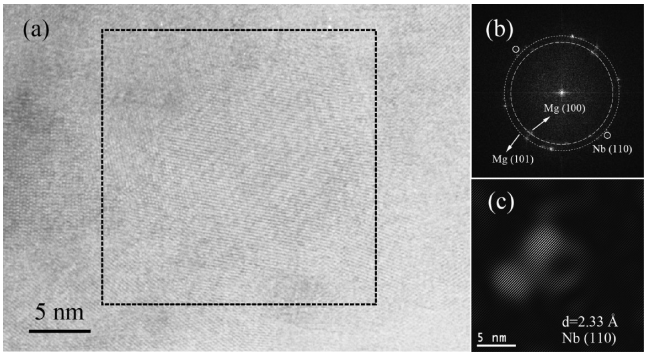


Figure 9. (a) High-resolution image, (b) FFT, and (c) IFFT images of the MgH_2 and 1 mol % Nb_2O_5 composite after dehydrogenation. The FFT area is marked by the square in panel a.

found in the FFT image shown in Figure 9b. In the IFFT image shown in Figure 9c, we can estimate the size of Nb as around 10 nm. All these observations indicate that the catalyst highly dispersed in the sample, with the size around 10−20 nm. The results well validated the Nb-gateway model in the MgH_2−Nb_2O_5 system. Tiny crystals of Nb act as the gateway through which hydrogen transports from MgH_2 to the outside.

The Mechanism of NbO-Catalyst. While strong interaction between MgH_2 and Nb_2O_5, as well as Nb, was confirmed, the unexpected stability of NbO is obscure. Considering NbO is hard to be pulverized during mechanical milling, this poor reactivity may be attributed to the size effect. Although a similar reaction, such as $MgH_2 + NbO \rightarrow NbH_2 + MgO$, is predicted by thermodynamics, large particle size and poor distribution of NbO limit the kinetics of the reaction. Therefore, NbO itself as the main phase is considered to have the catalytic effect, following some mechanism rather than the Nb-gateway model. In a recent study, NbO (111) was found to show effective catalytic activities,[22] which lend support to such consideration. On the other hand, TEM observations on NbO-doped composite also provide us with a hint to the mechanism of the catalytic effect. In the inset of Figure 10, single-crystal pattern of NbO, as well as $MgNb_2O_{3.67}$, has been indexed. The dark field image in Figure 10b was taken from $MgNb_2O_{3.67}$ (120). By comparing it with the corresponding bright field

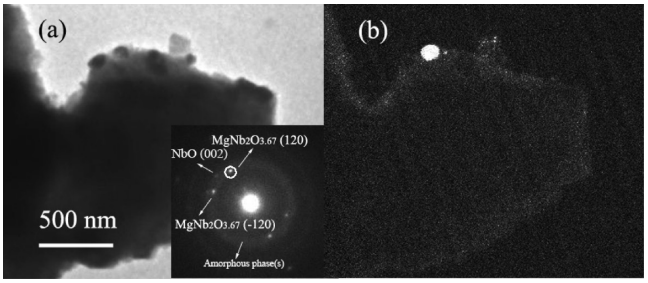


Figure 10. Typical TEM micrograph of the NbO-doped composite. (a) Bright field image. (b) Corresponding dark field image taken from the circled area.

image in Figure 10a, we can easily find out the single crystals of $MgNb_2O_{3.67}$, which show a dark contrast, with a size of ∼200 nm. In addition, a halo ring corresponding to an unknown amorphous phase(s), with the *d*-spacing range of 2.1−2.6 Å, was seen. It is implied that some reactions between MgH_2 and NbO, with poor kinetics, did occur during the milling process, forming $MgNb_2O_{3.67}$ and the unknown amorphous phase(s). As it was stated previously, the Mg−Nb−O phase was considered to help with hydrogen diffusion. It was pointed out that MgO is almost impermeable for hydrogen.[23] The Mg−Nb−O phase was proved able to absorb hydrogen[24] and even improve desorption properties of MgH_2 as a catalyst.[25] Here the existence of $MgNb_2O_{3.67}$ may provide pathways for hydrogen diffusion through the MgO scale covered on the surface of MgH_2, improving the desorption properties during dehydrogenation.

■ CONCLUSIONS

We were able to clarify the state of the Nb-contained catalysts in MgH_2 nanocomposites. Nb_2O_5 and Nb reacted with MgH_2 during the ball-milling process. NbH_2 and NbH, respectively, formed as the products of the reactions. During dehydrogenation, both NbH_2 and NbH decomposed into Nb and returned to the NbH state after rehydrogenation. It is suggested that both Nb_2O_5-doped and Nb-doped samples dehydrogenated following the Nb-gateway model in which Nb facilitates the hydrogen transportation from MgH_2 to the outside. On the other hand, reactions between NbO and MgH_2 were not confirmed. The promoted dehydrogenation may either be attributed to the catalytic effect of NbO itself or the existence of the $MgNb_2O_{3.67}$ phase. In addition, we found that the Nb_2O_5-doped sample tended to be refined in size, compared to the Nb-doped and NbO-doped ones, due to the hard and brittle features of Nb_2O_5. This size effect partially leads to a better dehydrogenation property in the sample. NbH_2 and Nb, with 10−20 nm in size, were also observed in the composite doped by 1 mol % Nb_2O_5, validating the Nb-gateway model in the MgH_2−Nb_2O_5 system. All the results reveal that tiny Nb crystals highly dispersed in the composites act as the essential catalyst and improve the desorption properties following the Nb-gateway model.

■ ASSOCIATED CONTENT

Supporting Information

The results for MgH_2 catalyzed by 1 mol % Nb_2O_5, 2 mol % Nb, 2 mol % NbO, as well as 2 mol % Nb and 5 mol % MgO, including dehydrogenation properties and morphology, can be found in the Supporting Information. This material is available free of charge via the Internet at http://pubs.acs.org/.

dx.doi.org/10.1021/jp4021883 | J. Phys. Chem. C 2013, 117, 10302−10307

AUTHOR INFORMATION

Corresponding Author

*E-mail: matao1984@hotmail.com (T.M.); isobe@eng.hokudai.ac.jp (S.I.).

Notes

The authors declare no competing financial interest.

ACKNOWLEDGMENTS

This work has been partially supported by HYDRO STAR (NEDO) and L-station (Hokkaido University).

REFERENCES

(1) Schlapbach, L.; Züttel, A. Hydrogen-Storage Materials for Mobile Applications. *Nature* **2001**, *414*, 353−358.

(2) Liang, G.; Boily, S.; Huot, J.; Neste, A. V.; Schulz, R. Mechanical Alloying and Hydrogen Absorption Properties of Mg−Ni System. *J. Alloys Compd.* **1998**, *267*, 302−306.

(3) Liang, G.; Huot, J.; Boily, S.; Neste, A. V.; Schulz, R. Catalytic Effect of Transition Metals on Hydrogen Sorption in Nanocrystalline Ball Milled MgH_2−Tm (Tm = Ti, V, Mn, Fe and Ni) Systems. *J. Alloys Compd.* **1999**, *292*, 247−252.

(4) Huot, J.; Pelletier, J. F.; Lurio, L. B.; Sutton, M.; Schulz, R. Investigation of Dehydrogenation Mechanism of MgH_2−Nb Nanocomposites. *J. Alloys Compd.* **2003**, *384*, 319−324.

(5) Pelletier, J. F.; Huot, J.; Sutton, M.; Schulz, R.; Sandy, A. R.; Lurio, L. B.; Mochrie, S. G. J. Hydrogen Desorption Mechanism in MgH_2−Nb Nanocomposites. *Phys. Rev. B* **2001**, *63*, 052103.

(6) Li, S.; Jena, P.; Ahuja, R. Dehydrogenation Mechanism in Catalyst-Activated MgH_2. *Phys. Rev. B* **2006**, *74*, 132106.

(7) Schimmel, H. G.; Huot, J.; Chapon, L. C.; Tichelaar, F. D.; Mulder, F. M. Hydrogen Cycling of Niobium and Vanadium Catalyzed Nanostructured Magnesium. *J. Am. Chem. Soc.* **2005**, *127*, 14348−14354.

(8) Oelerich, W.; Klassen, T.; Bormann, R. Metal Oxides as Catalysts for Improved Hydrogen Sorption in Nanocrystalline Mg-Based Materials. *J. Alloys Compd.* **2001**, *315*, 237−242.

(9) Barkhordarian, G.; Klassen, T.; Bormann, R. Fast Hydrogen Sorption Kinetics of Nanocrystalline Mg Using Nb_2O_5 as Catalyst. *Scr. Mater.* **2003**, *49*, 213−217.

(10) Barkhordarian, G.; Klassen, T.; Bormann, R. Effect of Nb_2O_5 Content on Hydrogen Reaction Kinetics of Mg. *J. Alloys Compd.* **2004**, *364*, 242−246.

(11) Yavari, A.; LeMoulec, A.; de Castro, F.; Deledda, S.; Friedrichs, O.; Botta, W.; Vaughan, G.; Klassen, T.; Fernández, A.; Kvick, Å. Improvement in H-Sorption Kinetics of MgH_2 Powders by Using Fe Nanoparticles Generated by Reactive FeF_3 Addition. *Scr. Mater.* **2005**, *52*, 719−724.

(12) Barkhordarian, G.; Klassen, T.; Bormann, R. Catalytic Mechanism of Transition-Metal Compounds on Mg Hydrogen Sorption Reaction. *J. Phys. Chem. B* **2006**, *110*, 11020−11024.

(13) Hanada, N.; Ichikawa, T.; Hino, S.; Fujii, H. Remarkable Improvement of Hydrogen Sorption Kinetics in Magnesium Catalyzed with Nb_2O_5. *J. Alloys Compd.* **2006**, *420*, 46−49.

(14) Hanada, N.; Hirotoshi, E.; Ichikawa, T.; Akiba, E.; Fujii, H. SEM and TEM Characterization of Magnesium Hydride Catalyzed with Ni Nano-particle or Nb_2O_5. *J. Alloys Compd.* **2008**, *450*, 395−399.

(15) Porcu, M.; Petford-Long, A.; Sykes, J. TEM Studies of Nb_2O_5 Catalyst in Ball-Milled MgH_2 for Hydrogen Storage. *J. Alloys Compd.* **2008**, *453*, 341−346.

(16) Friedrichs, O.; Sánchez-López, J.; López-Cartes, C.; Klassen, T.; Bormann, R.; Fernández, A. Nb_2O_5 "Pathway Effect" on Hydrogen Sorption in Mg. *J. Phys. Chem. B* **2006**, *110*, 7845−7850.

(17) Nielsen, T. K.; Jensen, T. R. MgH_2−Nb_2O_5 Investigated by In Situ Synchrotron X-ray Diffraction. *Int. J. Hydrogen Energy* **2012**, *37*, 13409−13416.

(18) Ma, T.; Isobe, S.; Morita, E.; Wang, Y.; Hashimoto, N.; Ohnuki, S.; Kimura, T.; Ichikawa, T.; Kojima, Y. Correlation between Kinetics and Chemical Bonding State of Catalyst Surface in Catalyzed Magnesium Hydride. *Int. J. Hydrogen Energy* **2011**, *36*, 12319−12323.

(19) Yao, H.; Isobe, S.; Wang, Y.; Hashimoto, N.; Ohnuki, S. Plastic Bag Method for Active Sample Loading into Transmission Electron Microscope. *J. Electron Microsc.* **2011**, *60*, 375−378.

(20) Yavari, A. R.; Vaughan, G.; Heunen, G. Structural Evolution and Metastable Phase Detection in MgH_2−5%NbH Nanocomposite During In-Situ H-Desorption in a Synchrotron Beam. *J. Alloys Compd.* **2003**, *353*, 246−251.

(21) Cullity, B.; Stock, S. *Elements of X-Ray Diffraction*, 3rd ed.; Prentice-Hall Inc., 2001.

(22) Takahashi, K.; Isobe, S.; Ohnuki, S. The Catalytic Effect of Nb, NbO and Nb_2O_5 with Different Surface Planes on Dehydrogenation in MgH_2: Density Functional Theory Study, *J. Alloys Compd.* **2013**, http://dx.doi.org/10.1016/j.jallcom.2013.02.044.

(23) Gonzalez, R.; Chen, Y.; Tsang, K. L. Diffusion of Deuterium and Hydrogen in Doped and Undoped MgO Crystals. *Phys. Rev. B* **1982**, *26*, 4637−4645.

(24) Rahman, M.; Livraghi, S.; Dolci, F.; Baricco, M.; Giamello, E. Hydrogen Sorption Properties of Ternary Mg−Nb−O Phases Synthesized by Solid-State Reaction. *Int. J. Hydrogen Energy* **2011**, *36*, 7932−7936.

(25) Rahman, M.; Castellero, A.; Enzo, S.; Livraghi, S.; Giamello, E.; Baricco, M. Effect of Mg−Nb Oxides Addition on Hydrogen Sorption in MgH_2. *J. Alloys Compd.* **2011**, *509S*, S438−S443.